In vivo evaluation of human skin anisotropy by polarization-sensitive optical coherence tomography

Shingo Sakai,[1,*] Masahiro Yamanari,[2] Yiheng Lim,[2] Noriaki Nakagawa,[1] and Yoshiaki Yasuno[2]

[1]*Innovative Beauty Science Laboratory, Kanebo Cosmetics Inc., Odawara, Kanagawa 250-0002, Japan*
[2]*Computational Optics Group, University of Tsukuba, Tennodai 1-1-1, Tsukuba, Ibaraki 305-8573, Japan*
**sakai.shingo@kanebocos.co.jp*

Abstract: We performed an *in vivo* three-dimensional analysis of anisotropic changes in the dermal birefringence of mechanically deformed human skin using polarization-sensitive optical coherence tomography (PS-OCT). The papillary-dermal birefringence of the forehead increased significantly when the skin was shrunk parallel to the body axis, and decreased significantly when the skin was shrunk perpendicular to the body axis. En-face images of the papillary-dermal birefringence revealed variations among individual subjects, and that both shrinking parallel to and stretching in perpendicular to the body axis promoted the formation of macro rope-like birefringent domains. We found that PS-OCT is useful for understanding anisotropic properties of collagen structure in the skin.

OCIS codes: (170.4500) Optical coherence tomography; (170.1870) Dermatology; (260.1440) Birefringence; (050.2555) Form birefringence; (110.4500) Optical coherence tomography

References and links

1. A. K. Langer, "On the anatomy and physiology of the skin. I. The cleavability of the cutis," Br. J. Plast. Surg. **31**(1), 3–8 (1978).
2. A. F. Borges, "Relaxed skin tension lines (RSTL) versus other skin lines," Plast. Reconstr. Surg. **73**(1), 144–150 (1984).
3. B. J. Wilhelmi, S. J. Blackwell, and L. G. Phillips, "Langer's lines: to use or not to use," Plast. Reconstr. Surg. **104**(1), 208–214 (1999).
4. C. J. Kraissl, "The selection of appropriate lines for elective surgical incisions," Plast Reconstr Surg (1946) **8**(1), 1–28 (1951).
5. H. T. Cox, "The cleavage lines of the skin," Br. J. Surg. **29**(114), 234–240 (1941).
6. T. Franco and G. Cotta-Pereira, "Histological basis of abdominal skin tension lines," An. Bras. Dermatol. **72**, 421–426 (1997).
7. J. Bush, M. W. Ferguson, T. Mason, and G. McGrouther, "The dynamic rotation of Langer's lines on facial expression," J. Plast. Reconstr. Aesthet. Surg. **60**(4), 393–399 (2007).
8. G. E. Piérard and C. M. Lapière, "Microanatomy of the dermis in relation to relaxed skin tension lines and Langer's lines," Am. J. Dermatopathol. **9**(3), 219–224 (1987).
9. T. Gibson, R. M. Kenedi, and J. E. Craik, "The mobile micro-architecture of dermal collagen: a bio-engineering study," Br. J. Surg. **52**(10), 764–770 (1965).
10. M. D. Ridge and V. Wright, "The directional effects of skin. A bio-engineering study of skin with particular reference to Langer's lines," J. Invest. Dermatol. **46**(4), 341–346 (1966).
11. P. Stoller, B. M. Kim, A. M. Rubenchik, K. M. Reiser, and L. B. Da Silva, "Polarization-dependent optical second-harmonic imaging of a rat-tail tendon," J. Biomed. Opt. **7**(2), 205–214 (2002).
12. T. Yasui, Y. Tohno, and T. Araki, "Characterization of collagen orientation in human dermis by two-dimensional second-harmonic-generation polarimetry," J. Biomed. Opt. **9**(2), 259–264 (2004).
13. T. Yasui, Y. Takahashi, S. Fukushima, Y. Ogura, T. Yamashita, T. Kuwahara, T. Hirao, and T. Araki, "Observation of dermal collagen fiber in wrinkled skin using polarization-resolved second-harmonic-generation microscopy," Opt. Express **17**(2), 912–923 (2009).
14. T. Yasui, Y. Takahashi, M. Ito, S. Fukushima, and T. Araki, "Ex vivo and *in vivo* second-harmonic-generation imaging of dermal collagen fiber in skin: comparison of imaging characteristics between mode-locked Cr:forsterite and Ti:sapphire lasers," Appl. Opt. **48**(10), D88–D95 (2009).

#150128 - $15.00 USD Received 29 Jun 2011; revised 2 Aug 2011; accepted 10 Aug 2011; published 16 Aug 2011

15. S. Y. Chen, H. Y. Wu, and C. K. Sun, "*In vivo* harmonic generation biopsy of human skin," J. Biomed. Opt. **14**(6), 060505 (2009).
16. A. M. D. Lee, H. Wang, Y. Yu, S. Tang, J. Zhao, H. Lui, D. I. McLean, and H. Zeng, "*In vivo* video rate multiphoton microscopy imaging of human skin," Opt. Lett. **36**(15), 2865–2867 (2011).
17. B. Cense, T. C. Chen, B. H. Park, M. C. Pierce, and J. F. de Boer, "*In vivo* birefringence and thickness measurements of the human retinal nerve fiber layer using polarization-sensitive optical coherence tomography," J. Biomed. Opt. **9**(1), 121–125 (2004).
18. M. Yamanari, M. Miura, S. Makita, T. Yatagai, and Y. Yasuno, "Phase retardation measurement of retinal nerve fiber layer by polarization-sensitive spectral-domain optical coherence tomography and scanning laser polarimetry," J. Biomed. Opt. **13**(1), 014013 (2008).
19. M. Miura, M. Yamanari, T. Iwasaki, A. E. Elsner, S. Makita, T. Yatagai, and Y. Yasuno, "Imaging polarimetry in age-related macular degeneration," Invest. Ophthalmol. Vis. Sci. **49**(6), 2661–2667 (2008).
20. B. H. Park, C. Saxer, S. M. Srinivas, J. S. Nelson, and J. F. de Boer, "*In vivo* burn depth determination by high-speed fiber-based polarization sensitive optical coherence tomography," J. Biomed. Opt. **6**(4), 474–479 (2001).
21. M. C. Pierce, J. Strasswimmer, B. H. Park, B. Cense, and J. F. de Boer, "Advances in optical coherence tomography imaging for dermatology," J. Invest. Dermatol. **123**(3), 458–463 (2004).
22. S. Sakai, M. Yamanari, A. Miyazawa, M. Matsumoto, N. Nakagawa, T. Sugawara, K. Kawabata, T. Yatagai, and Y. Yasuno, "*In vivo* three-dimensional birefringence analysis shows collagen differences between young and old photo-aged human skin," J. Invest. Dermatol. **128**(7), 1641–1647 (2008).
23. S. Sakai, N. Nakagawa, M. Yamanari, A. Miyazawa, Y. Yasuno, and M. Matsumoto, "Relationship between dermal birefringence and the skin surface roughness of photoaged human skin," J. Biomed. Opt. **14**(4), 044032 (2009).
24. M. Yamanari, S. Makita, and Y. Yasuno, "Polarization-sensitive swept-source optical coherence tomography with continuous source polarization modulation," Opt. Express **16**(8), 5892–5906 (2008).
25. Y. Lim, M. Yamanari, and Y. Yasuno, "Polarization sensitive corneal and anterior segment swept-source optical coherence tomography," Proc. SPIE **7550**, 75500O, 75500O-4 (2010).
26. M. Yamanari, S. Makita, V. D. Madjarova, T. Yatagai, and Y. Yasuno, "Fiber-based polarization-sensitive Fourier domain optical coherence tomography using B-scan-oriented polarization modulation method," Opt. Express **14**(14), 6502–6515 (2006).
27. G. Chinga, P. O. Johnsen, R. Dougherty, E. L. Berli, and J. Walter, "Quantification of the 3D microstructure of SC surfaces," J. Microsc. **227**(3), 254–265 (2007).
28. I. A. Brown, "Scanning electron microscopy of human dermal fibrous tissue," J. Anat. **113**(Pt 2), 159–168 (1972).
29. S. Jaspers, H. Hopermann, G. Sauermann, U. Hoppe, R. Lunderstädt, and J. Ennen, "Rapid *in vivo* measurement of the topography of human skin by active image triangulation using a digital micromirror device," Skin Res. Technol. **5**(3), 195–207 (1999).
30. T. Fujimura, K. Haketa, M. Hotta, and T. Kitahara, "Global and systematic demonstration for the practical usage of a direct *in vivo* measurement system to evaluate wrinkles," Int. J. Cosmet. Sci. **29**(6), 423–436 (2007).
31. L. T. Smith, K. A. Holbrook, and P. H. Byers, "Structure of the dermal matrix during development and in the adult," J. Invest. Dermatol. **79**(s1 Suppl 1), 93s–104s (1982).
32. S. Neerken, G. W. Lucassen, M. A. Bisschop, E. Lenderink, and T. A. Nuijs, "Characterization of age-related effects in human skin: A comparative study that applies confocal laser scanning microscopy and optical coherence tomography," J. Biomed. Opt. **9**(2), 274–281 (2004).
33. A. F. Borges, "Relaxed skin tension lines," Dermatol. Clin. **7**(1), 169–177 (1989).
34. P. Melis, M. L. Noorlander, C. M. van der Horst, and C. J. van Noorden, "Rapid alignment of collagen fibers in the dermis of undermined and not undermined skin stretched with a skin-stretching device," Plast. Reconstr. Surg. **109**(2), 674–680, discussion 681–682 (2002).
35. G. L. Grove, M. J. Grove, and J. J. Leyden, "Optical profilometry: an objective method for quantification of facial wrinkles," J. Am. Acad. Dermatol. **21**(3), 631–637 (1989).

1. Introduction

Visco-elasticity and anisotropy are important properties of the skin that relieve external forces. The anisotropy of the skin is important especially in the field of plastic surgery, because the direction of the incision influences scar formation. A practical method for understanding the skin's anisotropy has, therefore, been sought. Several types of skin lines including the Langer's line and relaxed skin tension lines have been proposed in the surgical field [1–3]. Langer created a map of the directions in which wounds created on the skin of human cadavers using a round tipped awl would be stretched, and these are called Langer's lines [1]. Langer's lines, however, are influenced by postmortem rigidity and not accurately applicable to living skin. Kraissl proposed lines called wrinkle lines, which are defined by tracing patients' wrinkles based on photographs [4]. He recognized that these lines were perpendicular to muscle action and scars in the wrinkles were least inconspicuous. However,

#150128 - $15.00 USD Received 29 Jun 2011; revised 2 Aug 2011; accepted 10 Aug 2011; published 16 Aug 2011

wrinkle lines are age dependent. Borges proposed the relaxed skin tension lines (RSTLs) [2]. These lines represent the direction of skin tension in a relaxed state, and are defined as follows. If the skin is pinched and then relaxed, a few deep linear furrows (RSTLs) perpendicular to the pinching direction are formed, while an S-shaped pattern is formed when the skin is not completely relaxed. Although wrinkle lines and the relaxed skin tension lines are considered to be the best guides for surgical incision [3], these lines do not perfectly agreed with each other. So far, we do not have a complete understanding of the anisotropic properties of *in vivo* skin tension.

It is commonly believed that skin anisotropy is due to the contraction of muscles [4] and the dermal structure, the directions of which determine anisotropic extensibility and elasticity of the skin. There are many reports regarding the relationship between dermal structure and skin lines. In the case of non-extension examination, Cox demonstrated that collagen fibers, a major dermal structural protein, run along Langer's lines [5]. Recently, however, some papers demonstrated that the relationship between the direction of collagen fibers and that of Langer's lines varies depending on the body site and motion [6,7]. Pierad *et al.* found thin elastic-like fibers, along the relaxed skin tension lines between collagen fibers [8]. Alternatively, in the case of extension examination, stretching the skin promotes the running of collagen fibers [9]. Redge demonstrated that stretching along Langer's lines promotes the running of collagen fibers more than stretching across them [10]. However, there are few reports regarding the anisotropic change of dermal structure under stretching along other directions than the Langer's line. So far, we do not completely understand the structural mechanism of skin anisotropy. The main difficulty lies in the histological approaches. In the reports described above, excision of the skin results in a disappearance of the skin's internal force. It is, therefore, important to make a noninvasive *in situ* analysis of the change of dermal structure.

Polarization-sensitive optical coherence tomography (PS-OCT) and second-harmonic-generation (SHG) microscopy are promising solutions for this problem. Their methodologies are not only *in vivo* and *in situ*, but also capable of visualizing depth-resolved collagen property. SHG-microscopy enables *in vivo* observation of dermal collagen fibers and analysis of its direction using the polarizing property of a SHG signal [11]. Yasui *et al.* described the evaluation of collagen fiber orientation using excised animal and human skin [12,13]. However, the dimension of the evaluated area was of the order of submillimeters, which might be too small to facilitate a discussion of the more macroscopic properties of the skin, such as Langer's lines and RSTLs. A few studies of *in vivo* observation of human skin using SHG microscopy have been reported [14–16]. However, there are no reports regarding *in vivo* investigation of collagen orientation. Alternatively, PS-OCT enables the three dimensional analysis of birefringence due to collagen fibers and has a wide transversal measurement area. PS-OCT has been widely applied to *in vivo* imaging in the ophthalmologic [17–19] and dermatological fields [20,21]. We have also evaluated the skin damage associated with photo-aging by measuring human dermal birefringence *in vivo* [22] and have reported the relationship between the progress of wrinkle and depth-dependent dermal birefringence in the crow's feet area *in vivo* [23]. In both studies, depth-resolved en-face birefringence maps showed the heterogeneous distribution of birefringence in the skin *in vivo* and it was indicated that this map would be useful for understanding skin anisotropy [22,23].

In this study, we further examine the birefringence property of *in vivo* human skin by PS-OCT, especially in order to understand skin anisotropy. The birefringence of human skin is investigated under several conditions of mechanical stress, i.e. stretching and compressing in several directions. This study can provide additional knowledge about the relationship between dermal properties and the above-mentioned skin lines including Langer's lines and RSTLs.

#150128 - $15.00 USD Received 29 Jun 2011; revised 2 Aug 2011; accepted 10 Aug 2011; published 16 Aug 2011

2. Materials and methods

2.1. Polarization sensitive optical coherence tomography

The technical details of PS-OCT employed in this study have been described in our previous papers [24,25]. The light source was a high-speed wavelength scanning light source with a center wavelength of 1310 nm, a scanning bandwidth of 110 nm, and a scanning speed of 30 KHz (HSL-2000, Santec, Japan). The probe power was 3.0 mW. The measured depth resolution in air was 10.2 μm, and the sensitivity was measured to be 105 dB. The transversal measurement range on the skin was 6 mm x 3.0 mm, which corresponds to 512 pixels x 256 pixels. The measurement time was about 5 seconds. After proper signal processing as described previously [24,26], we obtained the three-dimensional Jones matrix tomography of a sample. Polarization diversity OCT, also called backscattering intensity tomography and double-pass phase retardation tomography are derived from this Jones matrix tomography. Birefringence is defined as a local slope of the measured cumulative phase retardation along the depth [22,23]. To obtain the local slope, double-pass phase retardation was first moving-averaged by 30 axial pixels (93.5 μm) in depth. After automatic skin surface segmentation based on the back-scattering intensity image, the phase retardation data were realigned with respect to the surface. The local slope of the phase retardation was calculated by the linear-regression fitting method at two regions of 100-200 μm and 200-300 μm from the skin surface, which correspond to the papillary dermis and reticular dermis regions. This process was applied to all the A-scans of the OCT volume, and two en-face slope maps were obtained; papillary-dermal birefringence (PDB) map obtained at the 100-200μm depth region from the skin surface and reticular-dermal birefringence (RDB) map obtained at the 200-300μm depth region. The averaged papillary or reticular dermal birefringence was determined by averaging the slope values in the map. These maps were used for further texture analysis using Image J with SurfCharJ plugin (version 1c) [27] to understand the polarity of the birefringence distribution. This texture analysis provided a polar plot, which represents the preferred orientation of structure, and FAD (direction of azimuthal facets) of slope maps.

2.2. Human skin measurement protocol

Twenty-two Japanese male volunteers were recruited. The average age of the subjects was 54.3 ± 2.7 y/o (mean ± standard deviation) and ranged from 50 to 58 y/o. The center of the forehead was used as the target because forehead RSTLs and wrinkle lines are very clearly perpendicular to the body axis in this region.

A negative skin replica (25 mm x 25 mm) at the center of the forehead was taken by using SILFLO resin (Flexico Developments Ltd., England) and succeeded by OCT measurements. For OCT measurements, a custom-made instrument to quantitatively stretch or shrink the skin was attached to the skin by an adhesive tape as shown in Fig. 1. The center of the forehead (6 mm x 3 mm, 512 x 256 pixels), which was within the center window of the instrument and covered by the replicated region, was scanned by PS-OCT under stretching (23% in length) or shrinking (23% in length) conditions along parallel or perpendicular directions to the body axis. Although in some previous *in vitro* studies [9,28], the skin was stretched more largely, we selected the stretching amount of 23% because stretching of *in vivo* forehead skin perpendicular to the body axis more than 23% was with significant difficulty.

The surface profile of the negative replica was analyzed by fringe projection profilometer (Primos skin profilometer, GFMesstechnik GmbH, Berlin, Germany) [29,30]. This profilometer is based on the digital fringe projection technique where a fringe pattern is projected on the surface and the projection pattern is recorded by CCD. The analyzed field was an 18mm × 13mm area in the skin replica, of which the area of PS-OCT scan was located at the center. The surface profiles on five lines (10 mm long and 2 mm apart) around the center along the body axis were obtained. A built-in wave undulation removal filter (polynomial filter, Rank = 5) of Primos system software (Primos Ver.4.075) was applied. In

#150128 - $15.00 USD Received 29 Jun 2011; revised 2 Aug 2011; accepted 10 Aug 2011; published 16 Aug 2011

order to quantify the surface roughness of the skin, a roughness parameter, referred to as Ra, was determined. Ra is an arithmetic average value of profile peaks within the total measuring length, and a widely used parameter for wrinkle evaluation in cosmetic science. The details of this parameter are defined by the German standardization norm DIN EN ISO 4288 and ISO 4288 (1996). Written informed consent was obtained from all subjects before the measurement. The protocol conforms to the Helsinki Declaration and has been approved by the ethics committees of Kanebo Cosmetics, Inc. and the University of Tsukuba.

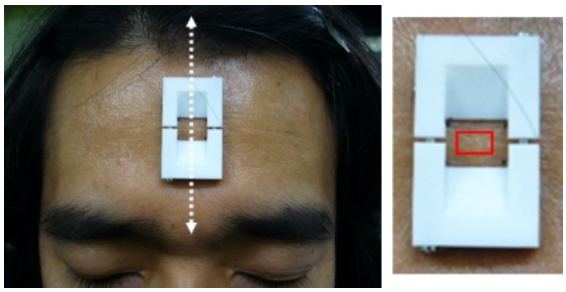

Fig. 1. Mechanical deformation of the forehead skin by the instrument

Broken-line arrows show the direction of the body axis. The area within red line was measured by PS-OCT.

2.3. Statistics

Repeated two-way analysis of variance (ANOVA) was applied in the case of papillary or reticular dermal birefringence separately. In the case of papillary dermal birefringence, there were significant interactions between the direction and the stretching condition (normal, stretching or shrinking) ($p<0.01$). After the two-way ANOVA, multiple group comparisons were performed with Bonferroni correction. There were no significant interactions between the direction and the stretching condition (normal, stretching or shrinking) of reticular dermal birefringence. Multiple group comparisons were performed with Bonferroni correction. The relationship between the change in dermal birefringence and Ra parameter was investigated using Pearson's correlation coefficients. Statistical analysis was performed using a statistics software SPSS (SPSS ver. 12.0j, SPSS Inc., IL).

3. Results and discussion

3.1. Dermal birefringence of relaxed forehead skin

Examples of the birefringence map of the forehead skin obtained from three subjects are shown in Fig. 2. The left column (Figs. 2a-2c) represents a PDB map, while the right column (Figs. 2d-f) represents an RDB map. In the PDB maps, ring-shaped domains (asterisks) and matrix domains (arrowheads) are evident. Some subjects showed clear rope-like domains in the matrix between ring-shaped domains perpendicular to the body axis (Fig. 2c.) though the appearance of this structure varied significantly among individual subjects. FAD values of the PDB and RDB map were found to be 89.4 ± 5.9 and 88.5 ± 10.2 degrees, respectively. These FAD values indicate that the forehead skin has an anisotropic structural flow of birefringence domains perpendicular to the body axis.

The heterogeneous distribution of birefringence found in PDB and RDB maps are consistent with our previous study [22]. The forehead skin lines are known to show clear direction, i.e., Langer's lines run parallel to the body axis (the direction of the arrow in Fig. 2) [1], while both wrinkle lines and the RSTLs run perpendicular to the body axis [2,4]. In general, the upper dermis consists of two layers, i.e., the papillary and reticular dermis [31]. The papillary dermis is a fine-collagen layer with a thickness of around 100μm [28,31,32], while the reticular dermis is a thick-collagen-bundle layer under the papillary dermis [28].

#150128 - $15.00 USD Received 29 Jun 2011; revised 2 Aug 2011; accepted 10 Aug 2011; published 16 Aug 2011

The en-face birefringence distributions of these two layers are represented by the PDB and RDB maps.

The ring-shaped domains are believed to be due to highly-layered collagen fibers in the peripheral regions of the infundibula, i.e., the epithelial invagination sites in the follicle [22]. The ring-shaped domains were clearer in the PDB maps than in the RDB maps. This is consistent with our understanding of this structure as infundibula.

The birefringence domains in the forehead ran roughly parallel to the direction of RSTLs and the wrinkle lines and perpendicular to the Langer's lines. Cox demonstrated that collagen fibers run along Langer's lines [5]. Langer's lines are, however, thought to be influenced by postmortem rigidity [2,3,33]. Collagen fibers did not always run in a direction corresponding to Langer's lines depending on their location [6]. Kraissl reported that the orientation of collagen fibers is parallel to wrinkle lines [4]. Dermal birefringence maps may show inner stress direction under normal conditions. More detailed clinical examination is called for in the future.

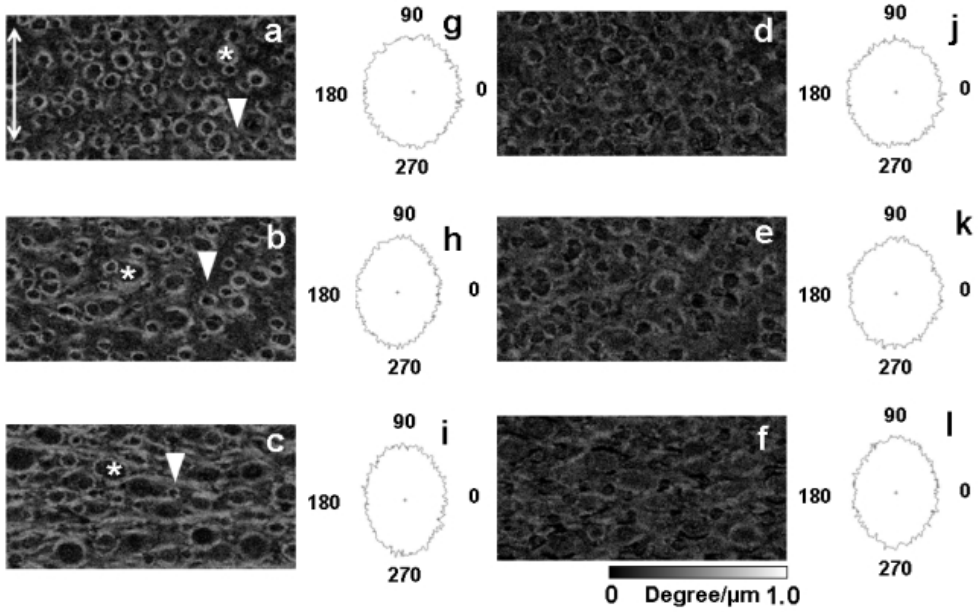

Fig. 2. En-face images of dermal birefringence distribution under normal conditions Examples from three subjects (a, g, d, j; b, h, e, k; c, I, f, l) are shown. The corresponding polar plot (g, h, i; j, k, l) was determined using the PDB (a, b, c) and RDB (d, e, f) maps, respectively. Arrows shows the body axis. Asterisks and arrow heads show papillary dermal birefringence from the peripheral region of the infundibula and between them, respectively.

3.2. Papillary-dermal-birefringence change under the deformation

We examined dermal-birefringence changes under deformation. Shrinking and stretching perpendicular to the body axis caused a d ecrease and increase in the papillary dermal birefringence, respectively as shown in Fig. 3a. According to Fig. 3b, stretching promoted a rope-like domain between the infundibula parallel to the stretching direction. By contrast, shrinking and stretching parallel to the body axis, i.e., parallel to the Langer's lines, promoted an increase and decrease in papillary dermal birefringence, respectively, as shown in Fig. 4a. Shrinking parallel to the body axis enhanced the contrast of the rope-like domain between the infundibula as seen in Fig. 4d. It is noteworthy that this contrast enhancement has also been observed under stretching conditions perpendicular to the body axis as shown in Fig. 3b. These results demonstrate that the *in vivo* forehead skin has a significant anisotropic property of papillary dermal birefringence.

#150128 - $15.00 USD Received 29 Jun 2011; revised 2 Aug 2011; accepted 10 Aug 2011; published 16 Aug 2011

It is known that the stretching of the skin promotes alignment of collagen fibers [9] [10,34]. We also speculate that internal force promotes the alignment of collagen fiber in the same direction, enhancing birefringence in this study. Gibson's study based on excised skin reported that stretching promotes alignment of reticular collagen fibers, not of papillary collagen fibers [9]. In contrast to these reports, our results demonstrated anisotropic change in dermal birefringence and anisotropic contrast enhancement of the rope-like domain. Since RSTLs of the forehead are known to be perpendicular to the body axis [2,33], our results can be interpreted to mean that stretching along the direction of RSTLs and shrinking perpendicular to them may enhance these birefringence features. This further suggests that stretching could promote alignment of papillary collagen fibers between infundibula. This disagreement regarding isotropy between our study and previous reports can be explained using the following reasons. (1) The previous studies used a light microscope to observe papillary dermal change. However, the structure of the collagen in the papillary dermis is too fine to be observed by a light microscope. (2) Excision of the skin, which was inevitable in the previous reports, released the inner stress of the skin. This could alter papillary dermal structure.

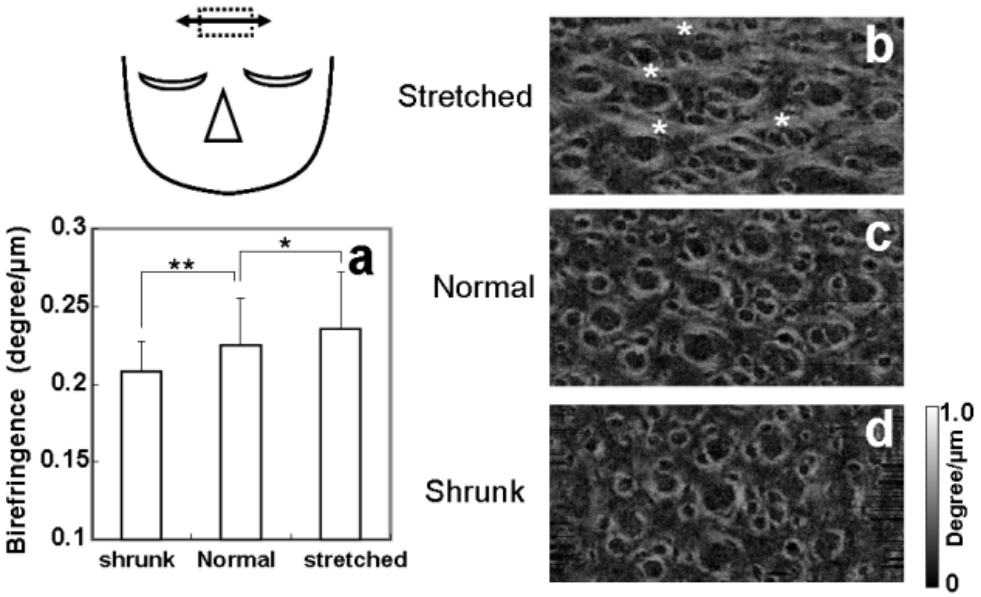

Fig. 3. Papillary-dermal-birefringence changes under deformation perpendicular to the body axis (a) A PDB map (b, c, d) was demonstrated under each condition. A macro rope-like structure was observed under stretching conditions (asterisks in b). *, $p<0.05$; **, $p<0.01$.

3.3. Reticular-dermal-birefringence change under deformation

In contrast to the papillary dermal birefringence, anisotropic change in reticular dermal birefringence by deformation was not found (Fig. 5). No statistical interaction between deforming direction and deformation state was found. *In vivo* stretching or shrinking condition may be not large enough to change the alignment of reticular collagen fibers for anisotropic birefringence change in this study. Stretching decreased reticular dermal birefringence, regardless of deformation direction.

This result and the results presented in section 3.2 suggest that the skin's inner stress may influence the alignment state of collagen fibers, and this effect has strong depth dependency. So far, some papers have used excised skin to report that stretching brings alignment of reticular collagen bundles [9,28]. In these studies, stretching was reported to be much greater

#150128 - $15.00 USD Received 29 Jun 2011; revised 2 Aug 2011; accepted 10 Aug 2011; published 16 Aug 2011

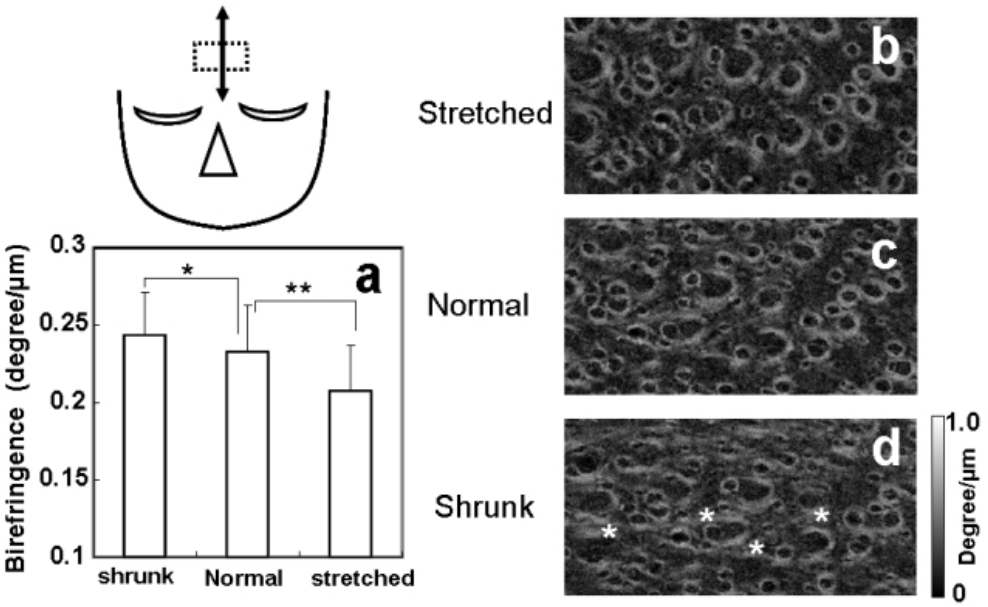

Fig. 4. Papillary-dermal-birefringence change under deformation parallel to the body axis (a) A PDB map (b, c, d) was demonstrated under each condition. A macro rope-like structure was observed under shrinking conditions (asterisks in b). *, $p<0.05$; **, $p<0.01$.

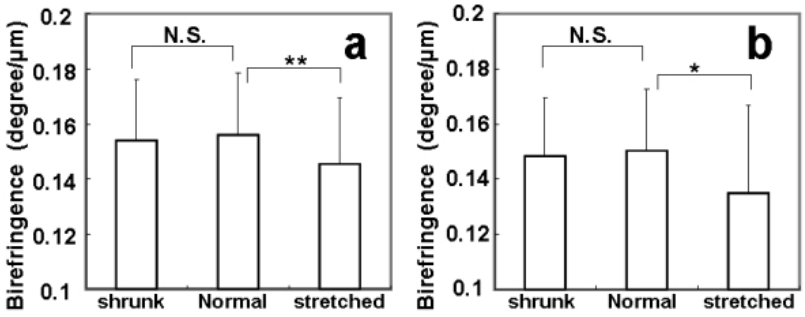

Fig. 5. Reticular-dermal-birefringence change under the deformation parallel (a) or perpendicular (b) to the body axis. *, $p<0.05$; **, $p<0.01$; N.S, non-significant

than our study (more than 40%). *In vivo* small stretching (23%) employed in our study may cause a smaller alignment of reticular collagen bundles.ar-dermal-birefringence change under deformation

In contrast to the papillary dermal birefringence, anisotropic change in reticular dermal birefringence by deformation was not found (Fig. 5). No statistical interaction between deforming direction and deformation state was found. *In vivo* stretching or shrinking condition may be not large enough to change the alignment of reticular collagen fibers for anisotropic birefringence change in this study. Stretching decreased reticular dermal birefringence, regardless of deformation direction.

This result and the results presented in section 3.2 suggest that the skin's inner stress may influence the alignment state of collagen fibers, and this effect has strong depth dependency. So far, some papers have used excised skin to report that stretching brings alignment of reticular collagen bundles [9,28]. In these studies, stretching was reported to be much greater than our study (more than 40%). *In vivo* small stretching (23%) employed in our study may cause a smaller alignment of reticular collagen bundles.

#150128 - $15.00 USD Received 29 Jun 2011; revised 2 Aug 2011; accepted 10 Aug 2011; published 16 Aug 2011

3.4. Relationships between papillary-dermal-birefringence change and wrinkle progression

The ratio of the birefringence under shrinking or stretching conditions to the birefringence under non-deforming, i.e. relaxed, conditions was determined in each direction. Only the birefringence change ratio in the parallel to the body axis under shrinking conditions (the condition of RSTLs formation) showed negative correlation to Ra as shown in Fig. 6.

Ra is a skin roughness parameter and is commonly used for the evaluation of wrinkle progression [23,30,35]. RSTLs of the forehead are known to run parallel to the wrinkle lines [2]. The increase in papillary dermal birefringence with RSTLs formation may show resistance to the formation of wrinkle lines under normal conditions in the case of forehead skin. The papillary dermal birefringence may not increase under pinching conditions in progressed wrinkles, because they may be stretched even under normal conditions.

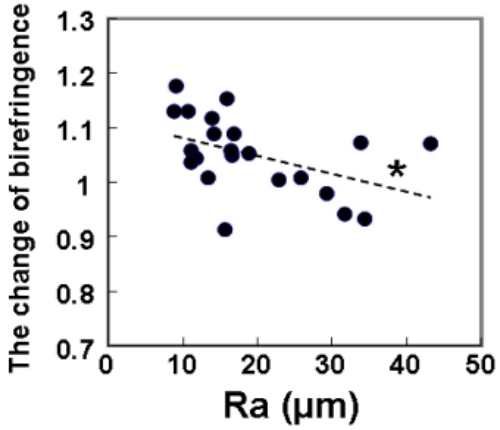

Fig. 6. Relationship between the change in papillary-dermal birefringence and Ra parameter under shrinking conditions parallel to the body axis. The change in papillary-dermal birefringence was the ratio of birefringence under shrinking conditions to birefringence under non-deforming conditions. *, $p<0.05$

4. Conclusion

We investigated the birefringence property of the dermis under mechanical stress using PS-OCT. It was found that the papillary dermal birefringence of the forehead skin has an anisotropic property. We concluded, therefore, that PS-OCT is useful for understanding the *in vivo* anisotropic properties of collagen structure and inner stress in the skin.

#150128 - $15.00 USD Received 29 Jun 2011; revised 2 Aug 2011; accepted 10 Aug 2011; published 16 Aug 2011